Inorg. Chem. **2006**, *45*, 1795–1804

Aqueous Spectroscopy and Redox Properties of Carboxylate-Bound Titanium

Ritika Uppal,[†] Christopher D. Incarvito,[†] K. V. Lakshmi,[‡] and Ann M. Valentine*[,†]

Department of Chemistry, Yale University, P.O. Box 208107, New Haven, Connecticut 06520-8107

Received October 4, 2005

The aqueous chemistry of Ti(III) and Ti(IV) in two different chemical environments is investigated given its relevance to environmental, materials, and biological chemistry. Complexes of titanium with the carboxylate ligands citrate and oxalate, found ubiquitously in Nature, were synthesized. The redox properties were studied by using cyclic voltammetry. All the titanium citrate redox couples are quasi-reversible. Electrospray mass spectrometry of the Ti(III) citrate solution shows the presence of a 1:2 Ti/cit complex in solution, in contrast to the predominant 1:3 Ti/cit complex with Ti(IV). The change in the coordination of the ligand to the metal on reduction may explain the quasi-reversible behavior of the electrochemistry. The redox potentials for Ti(IV) citrate in water vary with pH. At pH 7, the approximate $E_{1/2}$ is less than –800 mV. This stated change in redox properties is considered in light of the previously reported Ti(IV) citrate solution speciation. Analogous speciation behavior is suggested from the EPR spectroscopy of Ti(III) citrate aqueous solutions. The **g** tensors are deduced for several pH-dependent species from the simulated data. The X-ray crystal structure of a Ti^{III}_2 oxalate dimer $Ti_2(\mu\text{-}C_2O_4)(C_2O_4)_2(H_2O)_6 \cdot 2H_2O$ (**3**), which crystallizes from water below pH 2, is reported. Complex **3** crystallizes in a monoclinic $P2_1/c$ space group with $a = 9.5088(19)$ Å, $b = 6.2382(12)$ Å, $c = 13.494(3)$ Å, $V = 797.8(3)$ Å^3, and $Z = 2$. The infrared spectroscopy, EPR spectroscopy, and cyclic voltammetry on complex **3** are reported. The cyclic voltammetry shows an irreversible redox couple ~–196 mV which likely corresponds to the $Ti^{IV}_2/Ti^{III}Ti^{IV}$ couple. The EPR spectroscopy on solid complex **3** shows a typical $S = 1$ triplet-state spectrum. The solid follows non-Curie behavior, and the antiferromagnetic coupling between the two metal centers is determined to be –37.2 cm^{-1}. However, in solution the complex follows Curie behavior and supports a $Ti^{III}Ti^{IV}$ oxidation state for the dimer.

Introduction

The aqueous chemistry of Ti(III) and Ti(IV) is important to environmental, materials, medicinal, and biological chemistry. Titanium(IV), the predominant state in the presence of oxygen, is prone to hydrolysis to form the oxide, especially at neutral or basic pH values of the modern ambient oxidizing atmosphere. However, prevailing conditions over the history of the Earth may have featured elevated temperatures, anoxic environments, pH values as low as 2, and potentials as low as −500 mV.[1] Today, some locations, such as deep hydrothermal vents, provide significantly different environments. Even in the presence of dioxygen and near neutral pH, particularly hard ligands stabilize Ti(IV) against hydrolysis. Citrate and oxalate are two such ligands: they are of immense environmental and physiological importance and possess rich coordination chemistry. We undertook the current study as part of a larger exploration of the aqueous chemistry of titanium, with the consideration that diverse environmental conditions can give rise to different titanium chemistry.

Citric acid is present in human plasma as high as 0.1 mM and is an important chelator of hard metal ions.[2] Endogenous citrate coordinates Ti(IV) added to synovial fluid, mimicking Ti leaching from alloy implants.[3] Titanium(IV) citrate ruptures erythrocytes through interactions with the cell membrane.[4] Like some other titanium complexes,[5,6] Ti(IV)

* To whom correspondence should be addressed. E-mail: ann.valentine@yale.edu.
[†] Yale University.
[‡] Present address: Chemistry and Biochemistry Graduate Programs, The City University of New York, Staten Island, NY 10314.

(1) Williams, R. J. P.; Fraústo da Silva, J. J. R. *Natural Selection of the Chemical Elements*; Clarendon Press: Oxford, U.K., 1996.
(2) Martin, R. B. *J. Inorg. Biochem.* **1986**, *28*, 181−187.
(3) Silwood, C. J. L.; Grootveld, M. *Biochem. Biophys. Res. Commun.* **2005**, *330*, 784−790.
(4) Suwalsky, M.; Villena, F.; Norris, B.; Soto, M. A.; Sotomayor, C. P.; Messori, L.; Zatta, P. *J. Inorg. Biochem.* **2005**, *99*, 764−770.

10.1021/ic051714j CCC: $33.50
Published on Web 01/20/2006

citrate has anticancer properties.[7,8] In addition, Ti(IV) citrate delivers Ti(IV) to human serum transferrin.[9−12] The reduced form of Ti(IV) citrate, Ti(III) citrate, prepared in situ, is employed as a reductant for redox-active enzymes and in cell cultures.[13−16] In materials chemistry, Ti(IV) citrate is used in the controlled synthesis of titanium oxide materials via the Pechini process.[17] In most of the above cases, the Ti complexes are prepared in situ and their compositions not determined prior to use. Thus, there is an inconsistency between the utility of these complexes and the lack of rigorous characterization of their aqueous chemistry.

Structurally characterized complexes of Ti(IV) with citrate include an oxo−titanium complex with a Ti_8O_{10} core,[18] dinuclear and tetranuclear complexes with both peroxo and citrate ligands,[19,20] and dinuclear complexes with only citrate ligands.[21] Recently, mononuclear Ti(IV) complexes with three citrate ligands were isolated from aqueous solution.[21−24] The pH-dependent speciation of the mononuclear Ti(IV) complexes was characterized[24] and exploited for more favorable bioactivity.[12] To our knowledge, there are no X-ray crystal structures known for Ti(III) citrate complexes.

Oxalic acid, like citric acid, binds titanium. It facilitates the dissolution of Ti from the usually insoluble TiO_2, in a reaction that may mimic mineral weathering.[25] Oxalic acid is toxic to humans in high concentrations;[26] however, the oxalate ion may be involved in maintaining the ionic balance in plants, as it can form soluble and insoluble salts with alkali and alkaline earth metal cations.[27] Oxalates have been used as sacrificial electron donors in protein redox reactions.[16] Oxalic acid, even in the absence of metals, has rich redox chemistry. Its oxidation to carbon dioxide is an established reaction,[28] and oxalate can be reduced to glyoxylic and glycolic acid.[26] Oxalate−metal complexes are important in materials chemistry. The in situ preparation of titanium oxalate is used as a precursor in the preparation of barium titanate, which has excellent dielectric properties and is used in manufacturing ceramic capacitors.[29]

A number of Ti(III) oxalate complexes have been spectroscopically and/or crystallographically characterized. The earliest Ti(III) oxalate complexes to be characterized were $K[Ti(ox)_2]\cdot 2H_2O$, $NH_4[Ti(ox)_2]\cdot 2H_2O$, and $Ti_2(ox)_3\cdot 10H_2O$, where ox = $C_2O_4^{2-}$.[30] The crystal structure of $Ti_2(ox)_3\cdot 10H_2O$ revealed a terminal oxalate ligand on each metal ion, an oxalate ligand that is bridging and bidentate to each Ti, six coordinated waters, and four waters of crystallization.[31] A cesium bis(oxalate) complex $Cs[Ti(ox)_2(H_2O)_3]\cdot 2H_2O$[32] and a potassium tris(oxalate) complex $K_3[Ti(ox)_3(H_2O)]\cdot 4H_2O$[33] were also crystallographically characterized. In all of these complexes, oxalate acts as a bidentate ligand to Ti(III). A square-antiprismatic eight-coordinate polymeric Ti(III) complex was observed for the complex $NH_4[Ti(ox_2)]\cdot 2H_2O$, where eight oxalate oxygens bind each Ti and the oxalate molecules bridge different polyhedra.[34]

Several polynuclear Ti(IV) oxalates have also been reported. A dinuclear complex $Cs_4[TiO(ox)_2]_2\cdot 4H_2O$ features two metal centers connected by a bridging oxo.[35] Salts of Ti(IV) oxalate complexes $M_2[TiO(ox)_2]\cdot nH_2O$, where M = Li, Na, K, Rb, Cs,[36] and NH_4,[37] were synthesized. All have cyclic tetranuclear units with four oxygens of bidentate oxalate groups and two bridging oxo groups bound to each Ti center. An organometallic monomeric $Cp_2Ti(ox)$ has been characterized by X-ray crystallography.[38]

Ti(IV) is diamagnetic and cannot be observed by EPR spectroscopy. However, Ti(III) has a d^1 electronic state and its EPR spectra afford a sensitive probe of the environment surrounding the metal center.[39] The g values for Ti(III) EPR signals often vary over a fairly wide range ($g \sim 1.7-2.0$). Thus, EPR spectroscopy is a very useful probe of the

(5) Guo, Z. J.; Sadler, P. J. *Angew. Chem., Int. Ed.* **1999**, *38*, 1513−1531.
(6) Caruso, F.; Rossi, M. Antitumor Titanium Compounds and Related Metallocenes. In *Metal Ions in Biological Systems: Metal Complexes in Tumor Diagnosis and as Anticancer Agents*; Sigel, A., Sigel, H., Eds.; Marcel Dekker Inc.: New York, 2004; Vol. 42, pp 353−384.
(7) Abragam, D. *C. R. Hebd. Seances Acad. Sci.* **1935**, *200*, 990−991.
(8) Schwietert, C. W.; McCue, J. P. *Coord. Chem. Rev.* **1999**, *184*, 67−89.
(9) Sun, H.; Li, H.; Weir, R. A.; Sadler, P. J. *Angew. Chem., Int. Ed.* **1998**, *37*, 1577−1579.
(10) Messori, L.; Orioli, P.; Banholzer, V.; Pais, I.; Zatta, P. *FEBS Lett.* **1999**, *442*, 157−161.
(11) Guo, M.; Sun, H.; McArdle, H. J.; Gambling, L.; Sadler, P. J. *Biochemistry* **2000**, *39*, 10023−10033.
(12) Tinoco, A. D.; Valentine, A. M. *J. Am. Chem. Soc.* **2005**, *127*, 11218−11219.
(13) Zehnder, A. J. B.; Wuhrmann, K. *Science* **1976**, *194*, 1165−1166.
(14) Seefeldt, L. C.; Ensign, S. A. *Anal. Biochem.* **1994**, *221*, 379−386.
(15) Guo, M. L.; Sulc, F.; Ribbe, M. W.; Farmer, P. J.; Burgess, B. K. *J. Am. Chem. Soc.* **2002**, *124*, 12100−12101.
(16) Vincent, K. A.; Tilley, G. J.; Quammie, N. C.; Streeter, I.; Burgess, B. K.; Cheesman, M. R.; Armstrong, F. A. *Chem. Commun.* **2003**, 2590−2591.
(17) Cushing, B. L.; Kolesnichenko, V. L.; O'Connor, C. J. *Chem. Rev.* **2004**, *104*, 3893−3946.
(18) Kemmitt, T.; Al-Salim, N. I.; Gainsford, G. J.; Bubendorfer, A.; Waterland, M. *Inorg. Chem.* **2004**, *43*, 6300−6306.
(19) Kakihana, M.; Tada, M.; Shiro, M.; Petrykin, V.; Osada, M.; Nakamura, Y. *Inorg. Chem.* **2001**, *40*, 891−894.
(20) Dakanali, M.; Kefalas, E. T.; Raptopoulou, C. P.; Terzis, A.; Voyiatzis, G.; Kyrikou, I.; Mavromoustakos, T.; Salifoglou, A. *Inorg. Chem.* **2003**, *42*, 4632−4639.
(21) Deng, Y. F.; Zhou, Z. H.; Wan, H. L. *Inorg. Chem.* **2004**, *43*, 6266−6273.
(22) Zhou, Z. H.; Deng, Y. F.; Jiang, Y. Q.; Wan, H. L.; Ng, S. W. *Dalton Trans.* **2003**, 2636−2638.
(23) Kefalas, E. T.; Panagiotidis, P.; Raptopoulou, C. P.; Terzis, A.; Mavromoustakos, T.; Salifoglou, A. *Inorg. Chem.* **2005**, *44*, 2596−2605.
(24) Collins, J. M.; Uppal, R.; Incarvito, C. D.; Valentine, A. M. *Inorg. Chem.* **2005**, *44*, 3431−3440.
(25) Correns, C. W., Titanium. In *Handbook of Geochemistry*; Wedepohl, K. H., Ed.; Springer: Berlin, 1969−1978; Vol. 2, p 22-H-1.
(26) Hodgkinson, A. *Oxalic Acid in Biology and Medicine*; Academic Press: New York, London, 1977.
(27) Mahmut, C. *Turk. J. Zool.* **2000**, *24*, 103−106.
(28) Wiberg, K. B. *Oxidation in Organic Chemistry*; Academic Press: New York, London, 1965.
(29) Gao, L.; Xu, H. R. *J. Am. Ceram. Soc.* **2004**, *87*, 830−833.
(30) Eve, D. J.; Fowles, G. W. A. *J. Chem. Soc. A* **1966**, 1183−1184.
(31) Drew, M. G. B.; Fowles, G. W. A.; Lewis, D. F. *J. Chem. Soc. D, Chem. Commun.* **1969**, 876−877.
(32) Drew, M. G. B.; Eve, D. J. *Acta Crystallogr.* **1977**, *B33*, 2919−2921.
(33) Eve, D. J.; Niven, M. L. *Inorg. Chim. Acta* **1990**, *174*, 205−208.
(34) English, R. B.; Eve, D. J. *Inorg. Chim. Acta* **1993**, *203*, 219−222.
(35) Fester, A.; Bensch, W.; Trömel, M. *Inorg. Chim. Acta* **1992**, *193*, 99−103.
(36) Brisse, F.; Haddad, M. *Inorg. Chim. Acta* **1977**, *24*, 173−177.
(37) Van De Velde, G. M. H.; Harkema, S.; Gellings, P. J. *Inorg. Chim. Acta* **1974**, *11*, 243−252.
(38) Döppert, K.; Sanchez-Delgado, R.; Klein, H. P.; Thewalt, U. *J. Organomet. Chem.* **1982**, *233*, 205−213.
(39) Van Doorslaer, S.; Shane, J. J.; Stoll, S.; Schweiger, A.; Kranenburg, M.; Meier, R. J. *J. Organomet. Chem.* **2001**, *634*, 185−192.

coordination environment of Ti(III).[40] For dimeric Ti complexes, the study of EPR properties in frozen solution provides information about the ground state of the spin system, the separation between the metal centers, and the exchange overlap interaction between these metal centers. The EPR characteristics of complexes such as $(Cp_2Ti)_2(\mu$-phthalate) and $(Cp_2Ti)_2(\mu\text{-}OCH_3)_2$ have been studied extensively.[41−47] Most exhibit $S = 1$ triplet-state EPR spectra in a frozen solution indicating a zero field splitting characteristic of two interacting paramagnetic metal centers. The temperature dependence of the EPR spectra has been used to decipher the exchange coupling constants. Triplet-state EPR spectra of solutions containing $TiCl_3$ and carboxylate ligands such as EDTA and EGTA in a 2:1 mole ratio were used to support a dinuclear structure for the complexes.[48] In another study, the exchange coupling constant, J, for $Ti_2(ox)_3(H_2O)_6 \cdot 4H_2O$ was found to be -38 cm^{-1} (where $\hat{H} = -2J\hat{S}_A \cdot \hat{S}_B$).[49] This complex was later studied by variable-temperature magnetic susceptibility and the exchange coupling constant reported to be -60 cm^{-1}.[50]

The focus of the present investigation is the aqueous chemistry of complexes of Ti with the carboxylate donors citrate and oxalate. This study emphasizes the pH-dependent redox behavior and spectroscopic properties of Ti citrate and oxalate complexes. Aside from their relevance to biological and materials chemistry, the ligands were chosen because they afford access to the +4 and +3 oxidation states of Ti and to well-characterized monomers and dimers. The techniques used in this study, solid- and solution-state EPR spectroscopy, mass spectrometry, and electrochemistry, aptly characterize these aqueous Ti complexes. Under the conditions studied, titanium citrate is a mononuclear complex that is crystallographically characterized in the Ti(IV) oxidation state (structures **1** and **2** in Chart 1)[21−24] and titanium oxalate is a dimeric complex that is crystallographically characterized in the Ti^{III}_2 oxidation state (structure **3** in Chart 1) in which the two metal centers are connected by a bridging oxalate ligand. In this study, we also investigate the redox behavior of the Ti(IV) citrate system as a function of pH. The characterization of the redox properties represents important progress toward the full description of the aqueous coordination chemistry of Ti(IV) with citrate. The mass spectrometry provides evidence for the coordination of Ti(III) citrate. The study of the EPR spectral properties of Ti(III) citrate in solution as a function of pH elucidates the characteristics of different species existing at varying pH. EPR spectroscopy of the titanium oxalate dimer reveals information about the ground spin state, the exchange interaction, and the zero-field splitting parameters. The present investigation complements existing EPR data on the solid dimer, done at much higher temperatures,[49] and the variable-temperature magnetic susceptibility studies on a similar complex.[50]

Chart 1

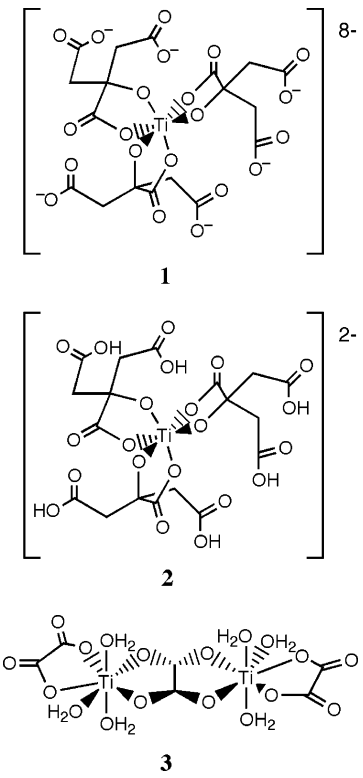

1 **2** **3**

Experimental Section

All aqueous solutions were prepared with Nanopure-quality water (18.2 MΩ cm resistivity; Barnstead model D11931 water purifier). Ti(IV) tris(citrate) ($Na_8[Ti(C_6H_4O_7)_3] \cdot 17H_2O$) (**1**) complex at pH ∼ 7 was crystallized by following a previously published procedure.[24] The Ti(IV) tris(citrate) ($K_2[Ti(C_6H_6O_7)_3] \cdot 4H_2O$) (**2**) was prepared at low pH by following the procedure of Zhou et al.[22]

Synthesis of (μ-Oxalato)hexaaquabis(oxalate)dititanium(III) Dihydrate, $Ti_2(\mu\text{-}C_2O_4)(C_2O_4)_2(H_2O)_6 \cdot 2H_2O$ (3). An 8.4 mL (12.5 mmol, 3 equiv) volume of N_2-purged 1.5 M oxalic acid ($H_2C_2O_4 \cdot 2H_2O$, Mallinckrodt) was added to 0.2 g (4.184 mmol, 1 equiv) of Ti wire (Aldrich), and the mixture was heated at 60 °C under N_2 with extremely slow stirring. The solution was then filtered to obtain brown crystals of **3**. The complex is sparingly soluble in water but dissolves in low concentrations with stirring. The complex is prone to oxidation in air. Yield: 0.091 g (43.3%). Elemental analysis was performed by Atlantic Microlabs (Norcross, GA). CH elemental analysis of $Ti_2C_6H_{16}O_{20}$. Found (calcd): C, 14.2 (14.29); H, 3.08 (3.17). UV (H_2O): $\lambda_{max} = 400$ nm ($\epsilon_{400\ nm} = 396$ M^{-1} cm^{-1}). Infrared spectra were collected in the form of a mull with Nujol

(40) Weil, J. A.; Bolton, J. R.; Wertz, J. E. *Electron Paramagnetic Resonance: Elementary Theory and Practical Applications*; Wiley: New York, 1994.
(41) Samuel, E.; Harrod, J. F.; Gourier, D.; Dromzee, Y.; Robert, F.; Jeannin, Y. *Inorg. Chem.* **1992**, *31*, 3252−3259.
(42) Francesconi, L. C.; Corbin, D. R.; Clauss, A. W.; Hendrickson, D. N.; Stucky, G. D. *Inorg. Chem.* **1981**, *20*, 2059−2069.
(43) Kramer, L. S.; Clauss, A. W.; Francesconi, L. C.; Corbin, D. R.; Hendrickson, D. N.; Stucky, G. D. *Inorg. Chem.* **1981**, *20*, 2070−2077.
(44) Francesconi, L. C.; Corbin, D. R.; Clauss, A. W.; Hendrickson, D. N.; Stucky, G. D. *Inorg. Chem.* **1981**, *20*, 2078−2083.
(45) Francesconi, L. C.; Corbin, D. R.; Hendrickson, D. N.; Stucky, G. D. *Inorg. Chem.* **1979**, *18*, 3074−3080.
(46) Fieselmann, B. F.; Hendrickson, D. N.; Stucky, G. D. *Inorg. Chem.* **1978**, *17*, 2078−2084.
(47) Fieselmann, B. F.; Hendrickson, D. N.; Stucky, G. D. *Inorg. Chem.* **1978**, *17*, 1841−1848.
(48) Cookson, D. J.; Smith, T. D.; Pilbrow, J. R. *J. Chem. Soc., Dalton Trans.* **1974**, 1396−1402.
(49) Povarova, N. V.; Sharov, V. A.; Krylov, E. I.; Olikov, I. I.; Shipilov, V. I.; Mokshin, V. M. *Russ. J. Inorg. Chem.* **1980**, *25*, 1854−1855.
(50) Wrobleski, J. T.; Brown, D. B. *Inorg. Chim. Acta* **1980**, 227−230.

Table 1. Crystallographic Data for $Ti_2(\mu\text{-}C_2O_4)(C_2O_4)_2(H_2O)_6 \cdot 2H_2O$ (**3**)

chemical formula	$C_6H_{16}O_{20}Ti_2$
formula weight	503.99
a (Å)	9.5088(19)
b (Å)	6.2382(12)
c (Å)	13.494(3)
α (deg)	90
β (deg)	94.64(3)
γ (deg)	90
V (Å^3)	797.8(3)
Z	2
space group	$P2_1/c$
T (K)	173(2)
radiatn (λ, Å)	Mo Kα (0.710 73)
D_{calcd} (g cm^{-3})	2.098
μ (cm^{-1})	11.15
R^a	0.0332[b]
$R_w{}^a$	0.0961[b]

[a] R values are based on F; R_w values are based on F^2; $R = \sum||F_o| - |F_c||/\sum|F_o|$ and $R_w = (\sum[w(F_o^2 - F_c^2)^2]/\sum w(F_o^2)^2])^{1/2}$. [b] For 1935 reflections with $I > 2\sigma(I)$.

between two NaCl plates on a Midac FT-IR spectrometer. IR (cm^{-1}): $\nu_{as}(CO_2)$ 1649, 1564; $\nu_s(CO_2)$ 1457, 1373; ν(Ti−O) 723.

X-ray Structure Determination. A brown block crystal of **3**, having approximate dimensions of 0.25 × 0.25 × 0.20 mm^3, was mounted with epoxy cement on the tip of a fine glass fiber. All X-ray crystallography measurements were made on a Nonius Kappa CCD diffractometer with graphite-monochromated Mo Kα radiation. The data were collected at a temperature of 173(2) K to a maximum 2θ value of 56.54°. The data frames were scaled and processed using the DENZO software package.[51] The data were corrected for Lorentz and polarization effects, and no absorption correction was applied. A total of 2891 reflections were collected of which 1935 were unique and observed ($R_{int} = 0.0209$). The structure was solved by direct methods and expanded using Fourier techniques.[52] The non-hydrogen atoms were refined anisotropically, and all hydrogen atoms were located from the residual electron difference map and refined with isotropic displacement parameters. Relevant crystallographic data are presented in Table 1.

Cyclic Voltammetry. The cyclic voltammograms were recorded on the potentiostat/galvanostat model 273 instrument (EG&G Princeton Applied Research). The voltammograms were visualized using the software "Echem" (EG&G Princeton Applied Research). The saturated calomel electrode was used as the reference electrode, the platinum electrode was the working electrode, and a platinum wire was used as the auxiliary electrode. In this study, all the potentials are reported vs NHE. A blank profile was acquired with a 0.1 M KNO_3 (Fisher, ACS-grade) solution that was used as the supporting electrolyte for all the experiments. The control voltammogram showed no oxidative or reductive peaks. A 2−4 mM solution of the complexes, containing 0.1 M KNO_3, was made in Nanopure water. The voltammograms were recorded at the scan rate of 30 mV s^{-1}. A scan range of 0 to −850 mV (vs SCE) was used for complex **1** and **2**, and +1 to −1 V (vs SCE) was used for complex **3**.

To study the pH dependence of Ti(IV) citrate electrochemistry, a 4 mM solution of complex **2** containing 0.1 M KNO_3 was prepared and the pH was increased slowly by addition of 1 M KOH. The cyclic voltammograms were recorded in the pH range 2−8, raising the pH in increments of 1. The final concentration at pH 8 was calculated to be 3.77 mM, so dilution due to the pH adjustment of the Ti(IV) citrate solution was minimal.

To study the voltammogram of titanium citrate beginning in the reduced state, a 33 mM Ti(III) citrate solution was prepared in situ by adding 39 mL of 0.1 M sodium citrate ($Na_3C_6H_5O_7 \cdot 2H_2O$, ACS-grade, Alfa-Aesar, 3.87 mmol) to 0.2 g of $TiCl_3$ (Aldrich, 1.29 mmol). The solution was stirred for 3 h, and the reaction mixture was diluted 10-fold before using it for the experiment. The voltammograms were recorded at pH 5.5 and 7.1 in the presence of 0.1 M KNO_3. The pH was increased using 1 M KOH (Sigma-Aldrich).

Sample Preparation for EPR Spectroscopy. A solution of Ti(III) citrate was prepared by following the procedure described above for the cyclic voltammetry. The sample was diluted to 3.3 mM in the presence of N_2, and the pH was adjusted with 1 M KOH or 1 M HCl solution. All Ti(III) citrate samples contained 20% glycerol (J. T. Baker) as a glassing agent. The samples were loaded into 4 mm quartz EPR tubes (Wilmad Glass).

For EPR of the solid complex **3**, the solid was crushed into fine powder, packed into a 4 mm quartz EPR tube, and frozen immediately in liquid nitrogen to prevent the oxidation of Ti(III) to Ti(IV). To conduct EPR spectroscopy measurements in solution, a 1−2 mM solution of the complex was prepared with 20% glycerol as the glassing agent. The mixture was immediately loaded into a 4 mm quartz EPR tube and frozen in liquid nitrogen.

EPR Spectroscopy. All EPR measurements on Ti(III) citrate were performed on an Elexys 500 EPR spectrometer (Bruker Instruments) operating at a frequency of 9.383 GHz, equipped with a TE_{102} cavity and a helium flow cryostat (Oxford Instruments). The EPR measurements were carried out at a temperature of 70 K. Typically two scans were collected/spectrum, under nonsaturating conditions, at a microwave power of 0.25 mW. The spectra were acquired at a modulation frequency of 100 kHz with a magnetic field modulation of 2 G. The center field of the EPR scans was set to 3450 G with a sweep width of 1000 G.

All EPR measurements on complex **3** were performed on a Varian E-9 EPR spectrometer (Varian Instruments) operating at a frequency of 9.239 GHz, equipped with a TE_{102} cavity and a helium flow cryostat (Oxford Instruments). The EPR measurements were carried out at temperatures ranging from 3.7 to 77 K, and typically 2−3 scans were collected/spectrum. The spectra were acquired at a modulation frequency of 100 kHz with magnetic field modulation of 4 G and microwave power of 2.0 mW. The center field for the EPR scans was set to 3300 G with a sweep width of 1000 G.

All spectral simulations were performed with the software package "Simfonia" (Bruker Instruments). The simulated and experimental EPR spectra were visualized using the program "WinEPR" (Bruker Instruments). The variable parameters in the spectral simulations (the g anisotropy, the zero-field splitting parameters, D and E, and the individual anisotropic line width components) were optimized to best reproduce the spectral features of the experimental spectra.

Mass Spectrometry. A concentrated solution of Ti(III) citrate was prepared by the addition of 2.9 mL of 2.5 M sodium citrate (7.2 mmol) to 0.37 g of $TiCl_3$ (2.4 mmol) under N_2. The solution was stirred for 4 h. The purple solution was filtered, and the electrospray mass spectrum was immediately collected on a Waters/Micromass ZQ spectrometer at a capillary voltage of 3 kV, cone voltage of 15 V, and extractor voltage of 3 V.

Results

Titanium Citrate. Electrochemistry. The cyclic voltammograms for aqueous solutions of titanium(IV) citrate were recorded at pH values ranging from 2 to 8. The cyclic

(51) Otwinowski, Z.; Minor, W. *Methods Enzymol.* **1997**, *276*, 307−326.
(52) Sheldrick, G. M. *Acta Crystallogr.* **1990**, *A46*, 467−473.

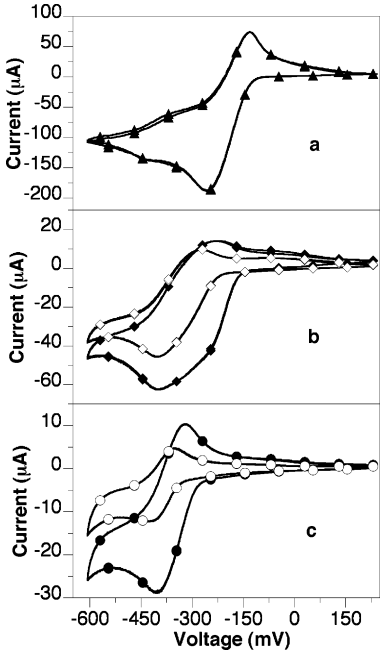

Figure 1. Cyclic voltammetric traces of 4 mM complex **2** in water as a function of pH shown vs NHE. Two overlaid scans are shown for each. Voltammograms are as follows:: (a) pH 2; (b) closed diamonds (◆), pH 3, open diamonds (◇), pH 4; (c) closed circles (●), pH 5, open circles (○), pH 6.

Table 2. Dependence of Redox Potential (vs NHE) of Ti(IV) Citrate Solution on pH

pH	E_{red} (mV)	E_{ox} (mV)	ΔE (mV)	$E_{1/2}$ (mV)
2	−258	−132	126	−195
3	−394	−230	164	−312
4	−405	−276	129	−341
5	−408	−320	88	−364
6	−427	−354	73	−391

voltammogram of a 2 mM solution of sodium citrate was acquired under similar conditions, as a control experiment, and it exhibited no peaks in the scan range used (data not shown). The cyclic voltammograms for Ti(IV) citrate solution in the pH range 2−6 are shown in Figure 1 and for pH 7 and 8 are shown in the Supporting Information (Figure S1). All the voltammograms for Ti(IV) citrate solutions were only quasi-reversible, and the $E_{oxidation}$, $E_{reduction}$, and approximate $E_{1/2}$ are given in Table 2. The peak current increased with the scan rate suggesting that the electrode reaction was a diffusion-controlled process, and the peak was not a result of an adsorption mechanism. The pH of the solution has a significant effect on the peak potentials and peak currents. The current and redox potentials decrease as the solution pH increases. The amplitude of the current observed in the voltammogram at pH 2 is much higher than the current observed in the other scans (Figure 1). The reason for this change could be either due to the decomposition of titanium citrate in solution, which has been previously reported in the literature,[21] or it may be related to the previously documented solution speciation (Figure S2).[24] Above pH 6, the redox reaction becomes very sluggish and no definite peaks are observed so that data cannot be interpreted. The redox potential of the system at or above pH 7 is beyond the range of the platinum working electrode,

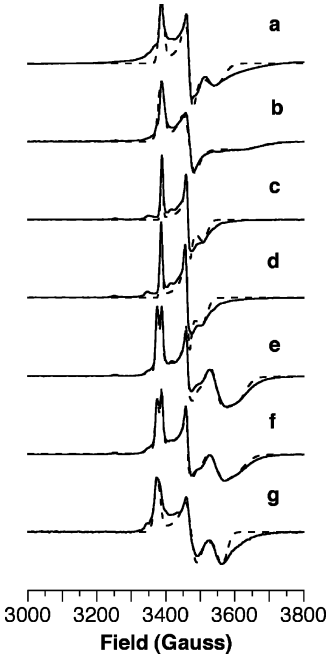

Figure 2. Experimental and simulated EPR spectra of Ti(III) citrate solution from pH 2−8 at a microwave power of 0.2524 mW: solid line, experimental spectra; dash line, simulated spectra. Key: (a) pH 2; (b) pH 3; (c) pH 4; (d) pH 5; (e) pH 6; (f) pH 7; (g) pH 8.

which is consistent with literature reports.[15,16] The voltammogram for complex **1**, crystallized at pH 7 and dissolved in water and 0.1 M KNO_3, resulting in a solution pH of 6.67, was analogous to the profile of the low pH form **2** adjusted to the same pH (Figure S3).

The apparent redox potentials decrease linearly between pH 3−6 (Figure S4) by 25 mV/pH unit. The value is less than the decrease of 59 mV/pH that would have indicated that the total number of protons and electrons involved in the charge transfer is the same and a Nernstian model is followed. Instead, this result indicates that population of different species (Figure S2), consistent with the speciation work,[24] contributes to the pH sensitivity of the redox potential. As the negative charge on each species increases with pH, it becomes harder to reduce and hence the reduction potential decreases. In the analogous experiment with catechol, $[Ti(catecholate)_3]^{2-}$ dominates the speciation between pH 6−12 and its reduction does not involve proton transfer, so its redox potential is constant over this range.[53]

The voltammograms were also recorded beginning in the reduced state for solutions of Ti(III) citrate generated in situ at pH 5.3 and 7. The pH 5.3 profile falls between the Ti(IV) citrate profiles of pH 5 and 6 closer to the pH 5 (Figure S5). The reaction at pH 7 is still sluggish but is similar to the voltammogram obtained for Ti(IV) citrate at the same pH (Figure S6).

EPR Spectroscopy. The EPR spectra of Ti(III) citrate solutions were collected from pH 2 to 8 and are shown in Figure 2. All spectra exhibit rhombic spectral features with the spectra at a few pH values indicating the presence of more than one species in solution. The EPR spectra at pH

(53) Borgias, B. A.; Cooper, S. R.; Koh, Y. B.; Raymond, K. N. *Inorg. Chem.* **1984**, *23*, 1009−1016.

Table 3. EPR Spectral Features of Ti(III) Citrate Solution at Different pH Values

pH	g_x	g_y	g_z
2	1.979	1.932	1.889
3	1.978	1.931	1.847
4	1.978	1.935	1.910
5	1.979	1.935	1.912
6	1.985	1.891	1.858
7	1.986	1.891	1.860
8	1.986	1.930	1.881

2−5 were simulated satisfactorily considering a single predominant species in solution. The **g** tensors were determined from the simulations and are presented in Table 3. The spectra at pH 6 and pH 7 must be attributed to the presence of two species in the sample. The spectra at pH 6 and 7 were each simulated by the addition of spectral contributions from a second species to the experimental spectrum at pH 5. Such a fit yields a signal that closely reproduces the experimental data. Table 3 also presents the **g** tensors for the additional new species in solution existing at pH 6 and 7.

The spectral features at pH 2 and pH 3 are distinct from the spectral features observed at other pH values. There is a small (<5%) contribution from the pH 2 species in the spectrum at pH 3, particularly visible in the *z*-component where a residual g_z peak from the pH 2 form is observed. The spectra at pH 4 and 5 are nearly identical with each other, except for a very small shift in the *g* values and minor changes in the line widths of the spectra. This resemblance suggests that the coordination may be similar at these pH values. The spectral features at pH 6 and pH 7 are a mixture of the pH 5 form (about 20%) and new species. The additional pH 6 and pH 7 components have almost identical *g* values. At pH 8, the spectral features change again with a different predominant species, possibly a mixed hydroxo.[24] The *g* values for the species at pH 8 are very different from those at lower pH, with the biggest change in the *z*-direction, suggesting that ligand exchange has its greatest effect along the g_z direction.

The spectra at pH 4−6 show interesting features, including some additional small peaks. This phenomenon has been observed for other mononuclear Ti(III) chelates and has been attributed to hyperfine couplings due to ^{49}Ti ($I = 7/2$) and ^{47}Ti ($I = 5/2$) isotopes.[48,54,55] The two sets of hyperfine structures overlap due to the comparable gyromagnetic ratios [$\gamma(^{49}\text{Ti})/\gamma(^{47}\text{Ti}) = 1.00026$].[56]

Mass Spectrometry. The electrospray mass spectrum of the in situ generated Ti(III) citrate in water at pH ∼ 4.6 shows the major peaks to be consistent with titanium isotope distributions for $Na_3[Ti(Hcit)_2]^+$ (peaks ∼ $m/z = 495$) and $Na_4[Ti(cit)(Hcit)]^+$ (peaks ∼ $m/z = 517$) (Figure 3). The free ligand peak was observed corresponding to $Na_3H(cit)^+$ ∼ m/z of 260 (data not shown). Small peaks were also observed consistent with the $Na_5[Ti(Hcit)_2(H_2cit)]^+$ (peaks ∼ $m/z = 731$) (Figure S7). Even though the peak for the 1:3 Ti/cit species is detected, the intensity of the peak is about 1/6 of the peak observed for the 1:2 species and, at the low signal: noise ratio, the isotope pattern also does not match completely. This result may suggest either the peak for the 1:3 species is a consequence of some oxidized Ti(IV) material in the Ti(III) citrate solution, resulting in complex **1** whose crystal structure was previously documented, or that both 1:2 and 1:3 species actually exist in the solution of the reduced form but most of the reduced complex is still the 1:2 Ti/cit species.

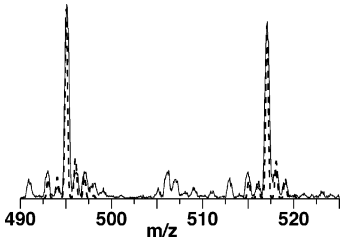

Figure 3. ESI-MS showing peaks consistent with titanium isotope distributions for $Na_3[Ti(Hcit)_2]^+$ (peaks ∼ $m/z = 495$) and $Na_4[Ti(cit)(Hcit)]^+$ (peaks ∼ $m/z = 517$).

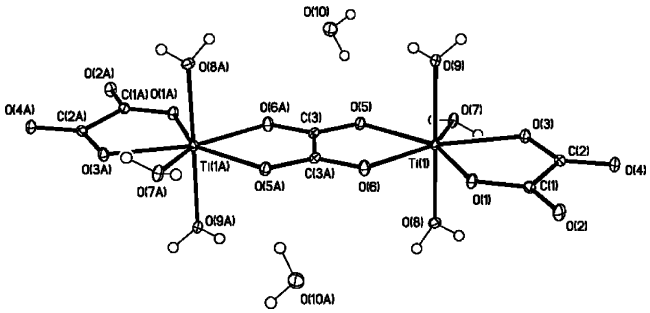

Figure 4. ORTEP diagram of $Ti_2(\mu\text{-}C_2O_4)(C_2O_4)_2(H_2O)_6{\cdot}2H_2O$.

Table 4. Selected Bond Lengths (Å) and Angles (deg) for Complex **3**

Ti−Ti	5.71	O(9)−Ti(1)−O(3)	86.16(6)
Ti(1)−O(9)	2.0528(14)	O(8)−Ti(1)−O(3)	93.21(5)
Ti(1)−O(8)	2.0544(13)	O(1)−Ti(1)−O(3)	73.85(5)
Ti(1)−O(1)	2.0673(14)	O(7)−Ti(1)−O(3)	71.43(5)
Ti(1)−O(7)	2.1369(14)	O(9)−Ti(1)−O(6)	92.79(6)
Ti(1)−O(3)	2.1379(14)	O(8)−Ti(1)−O(6)	90.70(6)
Ti(1)−O(6)	2.1513(13)	O(1)−Ti(1)−O(6)	71.65(6)
Ti(1)−O(5)	2.1717(13)	O(7)−Ti(1)−O(6)	143.48(6)
		O(3)−Ti(1)−O(6)	145.09
O(9)−Ti(1)−O(8)	174.77(6)	O(9)−Ti(1)−O(5)	85.19(6)
O(9)−Ti(1)−O(1)	97.01(6)	O(8)−Ti(1)−O(5)	92.05(5)
O(8)−Ti(1)−O(1)	87.78(5)	O(1)−Ti(1)−O(5)	145.60(5)
O(9)−Ti(1)−O(7)	90.59(6)	O(7)−Ti(1)−O(5)	70.12(5)
O(8)−Ti(1)−O(7)	84.30(6)	O(3)−Ti(1)−O(5)	140.41(5)
O(1)−Ti(1)−O(7)	143.81(6)	O(6)−Ti(1)−O(5)	73.95(6)

Titanium Oxalate 3. Description of the Crystal Structure of Complex 3. Complex **3** crystallizes in a monoclinic $P2_1/c$ space group with two molecules in the unit cell. The dimeric molecule resides on the center of inversion and is solvated by 2 waters of crystallization. The core structure of this complex is very similar to one which had a different unit cell and different number of waters of crystallization.[31] The ORTEP diagram for complex **3** is shown in Figure 4, and selected bond distances and angles are given in Table 4. The two titanium atoms have distorted pentagonal bipyramidal geometry and are connected by a bridging oxalate ligand. The terminal oxalate ligands bind asymmetrically to

(54) Watanabe, T.; Fujiwara, S. *J. Magn. Reson.* **1970**, *2*, 103−113.
(55) Symons, M. C. R.; Mishra, S. P. *J. Chem. Soc., Dalton Trans.* **1981**, 2258−2262.
(56) Jeffries, C. D. *Phys. Rev.* **1953**, *92*, 1262−1263.

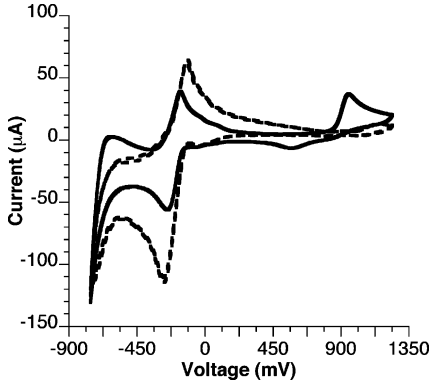

Figure 5. Cyclic voltammetric traces for 2 mM solution of oxalic acid (solid line) and complex **3** (dashed line). Voltages are shown vs NHE.

the Ti atoms with the Ti−O1/1A bond distance slightly shorter than the Ti−O3/3A distance.

The crystal lattice is held together by an extensive hydrogen-bonding network. All oxygen atoms with the exception of O(6) and O(6A) are involved in hydrogen bonding either themselves or through the hydrogens bound to them. The hydrogen atoms of O(7/7A/9/9A) interact with the oxalates of adjacent molecules and hydrogen atoms of O(8/8A) with the waters of crystallization. The O(2/2A/4/4A) hydrogen bond to the water ligands bound to the titanium atoms and O (3/3A/5/5A) bind to the protons on the waters of crystallization. Altogether, each titanium dimer interacts with four adjacent dimers and six molecules of cocrystallized water. All hydrogen bonds were determined to be below 2.2 Å.

FT-IR Spectroscopy. The FT-IR spectrum shows asymmetric carbonyl stretches between 1649 and 1564 cm^{-1} and symmetric stretches between 1457 and 1373 cm^{-1} (Figure S8). The carbonyl stretches are shifted to lower frequencies compared to free oxalic acid indicating deprotonated or metal-bound oxalic acid. The average difference between the asymmetric and symmetric stretches is ∼192 cm^{-1}. This value is intermediate between the generally observed separation for bridging carboxylates in ionic salts, which is typically less than 164 cm^{-1}, and the separation for a carboxylate binding in a monodentate fashion, which is generally more than 200 cm^{-1}.[57] The complex has one bidentate bridging oxalate and two terminal oxalates binding in a monodentate fashion. However, the carbonyl oxygens of the two terminal oxalates are hydrogen bonded to either water or oxalates on the adjacent molecules; hence, they are pseudobridging and that coordination could explain the intermediate value for the separation.

Cyclic Voltammetry. The cyclic voltammogram of oxalic acid alone in the range +1 to −1 V (vs SCE) shows an quasi-reversible redox couple with E_{red} at −250 mV and E_{ox} at −166 mV and an irreversible peak at 954 mV (Figure 5). The peak at 948 mV could be the result of oxalate oxidation and adsorption of CO_2 at the platinum electrode[58] or an impurity in the oxalic acid. The cyclic voltammogram of complex **3** in solution (pH ∼1.7) shows a irreversible redox couple with E_{red} at −274 mV and E_{ox} at −118 mV (Figure 5). The ΔE for the system is 156 mV, and the approximate $E_{1/2}$ is −196 mV vs NHE. This redox couple is most likely attributable to the $Ti^{IV}{}_2$ and $Ti^{III}Ti^{IV}$ dimer. Evidence for such a mixed-valence complex is confirmed by EPR studies on the dimer in the solid state and in solution (see below). The other redox couple, namely the $Ti^{III}Ti^{IV}$ to $Ti^{III}{}_2$, is likely more negative and is probably out of range of the platinum electrode employed in this study.

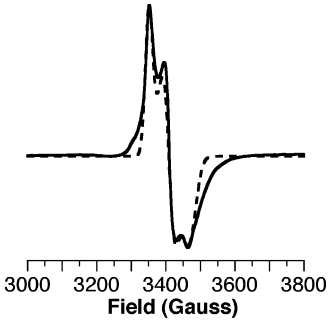

Figure 6. Experimental and simulated EPR spectrum for complex **3** in solution at 7 K.

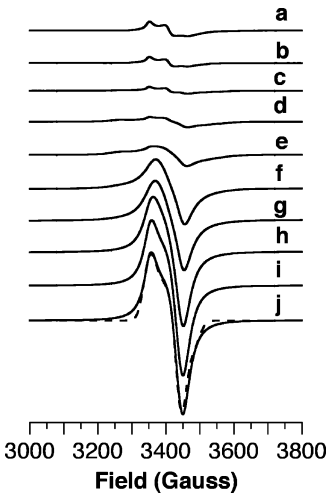

Figure 7. EPR spectra of solid complex **3** at different temperatures: (a) 3.7 K; (b) 7 K; (c) 15 K; (d) 20 K; (e) 24.7 K; (f) 35 K; (g) 40 K; (h) 50 K; (i) 60 K; (j) 65 K. The simulation of the spectrum at 65 K is included (dashed line).

EPR Spectroscopy. In frozen solution, complex **3** exhibits a typical rhombic $S = 1/2$ spectrum. The g values were interpreted from the simulated spectrum (Figure 6) as $g_x = 1.971$, $g_y = 1.936$, and $g_z = 1.901$. The optimized line widths for the x, y, and z components of the **g** tensor are 21, 29, and 37.4 G, respectively. As the temperature was increased above 30 K, the intensity of the signal decreased, as shown in Figure S9. The complex exhibits Curie behavior in solution (Figure S10), from 30 to 60 K, which validates the $S = 1/2$ ground-state assignment.

The EPR spectrum of the solid dimer at temperatures less than 20 K displays features characteristic of the rhombic spectrum of the frozen solution (Figure S11). But, as the temperature is increased above 20 K, a triplet-state EPR spectrum is observed. The EPR spectra for the solid complex **3** at different temperatures are shown in Figure 7. The

(57) Deacon, G. B.; Phillips, R. J. *Coord. Chem. Rev.* **1980**, *33*, 227−250.
(58) Berná, A.; Rodes, A.; Feliu, J. M. *J. Electroanal. Chem.* **2004**, *563*, 49−62.

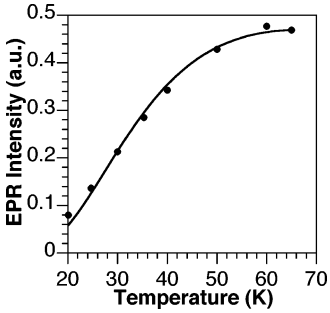

Figure 8. EPR intensity vs temperature plot for solid complex **3**.

spectrum displays an axial $S = 1$ spectrum with $g_x = 1.945$ and $g_y = g_z = 1.93$ and zero-field splitting parameters, D and E, of 0.001 77 and 0.003 36 cm^{-1}, respectively. The g values and zero-field splitting parameters were determined from the simulated spectrum shown in Figure 7j. The individual line widths were optimized to 34, 34, and 36 G for the x, y, and z components of the **g** tensor, respectively, to reproduce the experimental spectrum. In this case, a typical spin polarized six line triplet state EPR spectrum is not detected as the values of D and E are very small and the signal is inhomogeneously broadened.[40] Contrary to the observations in the frozen solution, the solid dimer follows non-Curie behavior which is additional evidence against an $S = 1/2$ spin ground state for this species. The intensity data plotted as a function of temperature display an exponential increase in the intensity with temperature (Figure 8). The isotropic exchange interaction J can be determined from the temperature dependence of the EPR signal intensity according to the equation

$$I_{EPR} = (A/T - \Theta)\left[1 + \frac{1}{3}\exp(-2J/kT)\right]^{-1}$$

where Θ is the Weiss constant.[41] From the least-squares fit of the EPR spectral data for the solid dimer to the above equation, the values of J and A were determined to be -37.2 cm^{-1} and 83.654 K^{-1}, respectively. The negative value of J indicates that the two Ti(III) centers are antiferromagnetically coupled to each other.

Discussion

Titanium Citrate. Although reduction of biomolecules by Ti(III) citrate has found widespread applications, the redox properties of Ti(III) citrate are poorly defined. Earlier reports have quoted the Ti(IV)/Ti(III) redox potential to be around -480 mV vs NHE,[13,59] and this estimate is based on older literature.[60] In the latter, though, the redox potential was reported versus the normal calomel electrode and was not adjusted. One study states that Ti(III) citrate takes up one proton upon reduction, with $E_{m,7.0} = -500$ mV vs NHE and $\Delta E/\Delta pH = -60$ mV at 25 °C.[59] This potential has been questioned recently; on the basis of the ability of Ti(III) citrate to reduce bipyridinium salts,[15] the value is estimated as <-800 mV.[15,16] In all of these cases, the Ti(III) citrate is prepared in situ, usually from $TiCl_3$ and 1 to 1.2 equiv of citrate. The speciation of the Ti(IV) ion with citrate suggests that, with fewer than 3 equiv of citrate, a mixture of oxo and hydroxo species occurs.[24] A similar condition may hold for the Ti(III) ion, and we entertained the possibility that, with a higher citrate/metal ratio, the system might prove more tractable. In the current work, the speciation of at least the oxidized species is known, and still, as reported,[15,16] the voltammograms are not fully reversible and the potential is very low. The mass spectrometry of the Ti(III) citrate solution prepared in situ at pH $\sim$ 4.6 with 1:3 metal/citrate ratio provides evidence for a change in ligand coordination after the reduction of Ti. The spectrum suggests that Ti(III) in its reduced state predominantly forms a complex with only 2 molecules of citrate. This kind of coordination has been observed for metals such as Fe(III)[61] and Al(III),[62] where one of the β-carboxylates on each citrate also binds the metal, making each a tridentate ligand. The quasi-reversibility of the cyclic voltammograms are likely a consequence of the change in coordination of Ti upon reduction.

The redox potential of Ti(IV) citrate solution was studied from pH 2 to 8. All of the redox potentials for the Ti(IV)/Ti(III) couple are lower than the formal potential of the couple in acid which is slightly positive (+0.099 V vs NHE).[53] The hard ligands that prevent hydrolysis and serve to keep Ti in solution also favor the oxidized form, lowering the redox potential. The reduction potential of the Ti(IV) tris(catecholate), for example, has been measured with a dropping mercury electrode to be -1.14 V.[53] The approximate half-wave potential for the citrate complex decreased greatly from pH 2 to pH 3 and slowly thereafter until pH 8, a result that can be explained by taking into account the speciation of Ti(IV) citrate in solution. The change with pH is less than one would expect for reduction with proton uptake (see above). At pH 2, the dominant complex is a 1:1 Ti(IV)/citrate species, but as the pH is increased to 3, a 1:3 Ti/citrate species forms and predominates, with sequential deprotonation of the dangling carboxylates, until pH 8 (Figure S2). This deprotonation changes the overall charge on the complex, from a $2-$ species at low pH to an $8-$ species by pH 7. This speciation may explain the decrease in the redox potential with pH.

These values of approximate half-wave potential are comparable to the reported value of -600 mV vs SCE (Figure S2) (-358 mV vs NHE), determined for a solution of the complex crystallized at pH $\sim$ 6, assuming the pH of the solution of the complex would be close to that value.[23] These results are also in agreement with the suggestion that the redox potential of Ti(IV) citrate at neutral pH is less than -800 mV.[15]

The depletion of current as the pH increases could also be explained by the same solution speciation. The speciation

(59) Holliger, C.; Pierik, A. J.; Reijerse, E. J.; Hagen, W. R. *J. Am. Chem. Soc.* **1993**, *114*, 5651−5656.
(60) Strubl, R. *Collect. Czech. Chem. Commun.* **1938**, *10*, 475−492.
(61) Matzapetakis, M.; Raptopoulou, C. P.; Tsohos, A.; Papaefthymiou, V.; Moon, N.; Salifoglou, A. *J. Am. Chem. Soc.* **1998**, *120*, 13266−13267.
(62) Matzapetakis, M.; Kourgiantakis, M.; Dakanali, M.; Raptopoulou, C. P.; Terzis, A.; Lakatos, A.; Kiss, T.; Banyai, I.; Iordanidis, L.; Mavromoustakos, T.; Salifoglou, A. *Inorg. Chem.* **2001**, *40*, 1734−1744.

diagram for Ti(IV)-containing species (Figure S2) suggests that the principal Ti(IV) citrate complex at pH 2 ($[Ti(Hcit)]^+$) is positively charged so it may be easier for it to approach the reducing electrode, while the predominant species are negatively charged at pH 3 and above.[24] The negative charge on the complex increases as the solution pH rises making the approach and surface reaction at the electrode more disfavored. It is understandable that a species with a charge as high as −8 would be very difficult to reduce.

The cyclic voltammogram starting with the Ti(III) citrate solution at pH 7 is similar to the profile of Ti(IV) citrate solution at the same pH and to the voltammogram of complex **1** dissolved in water. Also, the voltammogram starting with Ti(III) citrate at pH 5.3 lies between the Ti(IV) citrate profiles of pH 5 and 6. This result suggests that the in situ generated reduced species at different pH are related or at least rapidly interconverting species.

Additional insight into the speciation of the Ti(III) complex in solution is provided by EPR spectroscopy. The EPR spectral features of the Ti(III) complex in solution at pH 2.0 are completely different from the spectral features observed at other pH values, especially in the g_z tensor component. These differences may be rationalized by the occurrence of a very different chemical species in solution at pH 2.0. At pH 4 and 5, the EPR spectra for the Ti(III) species in solution show similar features indicating that the coordination geometry of the two species existing at these pH values is comparable, as is true for the Ti(IV) species.[24] The predominant species at these pH values for Ti(IV) differ only by the deprotonation of the citrate dangling carboxylates. At pH 6−7, species emerge for the Ti(III) complex in solution with similar g values and nearly identical EPR spectra. One or both of these new species may correspond to reduced **1**. There is ∼20% contribution from the pH 5 form to the EPR spectrum of the Ti(III) species at pH 6 and 7. At pH 8, the EPR signal shows the presence of a new Ti(III) species, which is again consistent with the Ti(IV) speciation since mixed hydoxo species start forming at this pH. Even though distinguishable Ti(III) species exist at each pH, ranging from 2 to 8, the **g** tensors for all the species are less than 2.0. This result indicates that the unpaired electron lies in a nonbonding orbital which in this case would be one of the t_{2g} orbitals assuming idealized octahedral geometry and is mixing with the unfilled d-orbitals in its vicinity.[63]

The identities of these components in the reduced state, as well as their stability constants, remain to be determined. Taken together, the pH dependence of the redox and EPR behavior of Ti citrate in solution agrees well with the spectropotentiometric studies in the oxidized state and suggests strongly that a similar richness of speciation holds for the reduced state.

Ti Oxalate Dimer 3. The X-ray crystal structure and IR spectroscopy of complex **3** agree with the presence of one bridging and two terminal oxalates. The Ti oxalate complex has a core structure similar to one reported earlier,[31] but it crystallizes in a different unit cell and with different number of waters of crystallization. The cyclic voltammetry for complex **3** in water showed an irreversible redox couple with an apparent $E_{1/2}$ of −196 mV. The redox potential of Ti^{3+}/TiO^{2+} couple in oxalic acid media was estimated to be ∼0 V vs NHE.[64] The current redox potential is lower than reported earlier but at that time the above couple was assumed, and the presence of a titanyl moiety in the present case has not been demonstrated. This redox couple is most likely due to a dimer.

The EPR spectrum of complex **3** in solution shows a typical $S = 1/2$ rhombic EPR spectrum which follows Curie behavior. This spectrum may result from a mixed-valence $Ti^{III}Ti^{IV}$ dimer or from dissociated Ti(III) monomers. Some oxidation can be observed because the complex loses its orange color upon oxidation. Although the samples still had substantial orange color before freezing, it is possible that some molecules were oxidized resulting in this spectrum. The remaining intact Ti^{III}_2 dimer is EPR silent, suggesting that it is antiferromagnetically coupled. The excited triplet state spectrum is not observed in solution, probably because even though there is a possibility of excitation of higher spin manifolds at higher temperatures, in solution the relaxation time of the triplet state is too small. This short relaxation time results in broadening of the signal so that no signal is observed.

The EPR spectrum of the solid is more complex. At low temperatures, it shows a small population having the same rhombic spectrum as in frozen solution which is attributed to a small number of oxidized $Ti^{III}Ti^{IV}$ dimers in the solid. The similarity of this species to the one in solution suggests that the solution species may also be a dimer. But as the temperature is increased above 20 K, the spectral features are dramatically altered. The new signal is typical of an axial $S = 1$ spectrum with a contribution from the zero-field splitting parameters, D and E, 0.001 77 and 0.003 36 cm^{-1}, respectively. The axial spectrum at higher temperatures is a consequence of the magnetic interaction between the two metal centers of the Ti^{III}_2 dimers. Thus, at low temperature, the antiferromagnetic coupling between the two titanium centers of the Ti^{III}_2 dimer results in an $S = 0$ state and only the signal corresponding to the small number of oxidized $Ti^{III}Ti^{IV}$ dimers is observed. At higher temperatures, the higher spin manifolds are excited and the $S = 1$ signal from the Ti^{III}_2 dimers is detected. The exchange interaction J for the system from the intensity versus temperature (Figure 8) plot, using the $S = 1$ signal at temperatures above 20 K, was determined to be -37.2 cm^{-1}. This value of J corresponds well with the earlier literature on Ti^{III}_2 dimers as shown in Table 5. The J value for complex **3** falls between the complexes with the Ti−Ti distance of 4.1 and 6.2 Å and is comparable to that reported for the similar complex with 4 molecules of waters of crystallization.[50]

X-ray crystallography is not very sensitive to the distance changes due to change in oxidation state, especially due to averaging if one Ti were in the +3 oxdiation state and the other in the +4 oxidation state. To explore the possibility

(63) Raynor, J. B.; Ball, A. W. L. *Inorg. Chim. Acta* **1973**, *7*, 315−318.

(64) Pecsok, R. L. *J. Am. Chem. Soc.* **1951**, *73*, 1304−1308.

Table 5. Comparison of Structural and EPR Properties for Ti^{III}_2 Dimers

complexes	Ti−Ti (Å)	J (cm^{-1})	ref
$(Cp_2Ti)_2(\mu$-terephthalate)	10.6	−0.7	44
$(Cp_2Ti)_2(\mu$-isophthalate)	9.2	−1.4	44
$(Cp_2Ti)_2(\mu$-phthalate)	6.2	−2.8	44
$Ti_2(\mu$-$C_2O_4)(C_2O_4)_2(H_2O)_6 \cdot 2H_2O$ (**3**)	5.7	−37.2	this work
$Ti_2(\mu$-$C_2O_4)(C_2O_4)_2(H_2O)_6 \cdot 4H_2O$		−38, −60[a]	49, 50
$[(CH_3Cp)_2Ti]_2(\mu$-$Br)_2$	4.123	−138[a]	65
$[(CH_3Cp)_2Ti]_2(\mu$-$Cl)_2$	3.926	−160[a]	65
$(Cp_2Ti)_2(\mu$-$OCH_3)_2$	3.35	−268	41

[a] For these data, J values were calculated from magnetic susceptibility experiments.

that the $S = 1$ triplet state could be a result of the intermolecular coupling of spins from two different $Ti^{III}Ti^{IV}$ dimers, the concentration dependence of the spectral feature was investigated (data not shown). The line widths of the spectral features did not change with the doubling of the concentration, which indicates that the relaxation mechanism is only due to intramolecular interactions; i.e., coupling arises from the two Ti centers of the same dimer, indicating a Ti^{III}_2 dimer in the solid state. This relaxation is probably a result of spin−orbit coupling or the anisotropies in the **g** tensor.

Conclusion

The redox and EPR properties of two titanium complexes with significantly different coordination environments were investigated. Ti(IV) citrate is a monomer with an octahedral structure, and Ti^{III}_2 oxalate is a dimeric complex with each titanium in a pentagonal bipyramidal environment. The approximate half-wave potentials for the Ti(IV)/Ti(III) redox couples for both complexes were found to be negative. For example, the redox potential for Ti citrate solution at the current biologically relevant pH was found to be less than −800 mV vs NHE so current environmental conditions would not make this reduction likely. On the other hand, the $Ti^{IV}_2/Ti^{III}Ti^{IV}$ oxalate and Ti(IV)/Ti(III) citrate redox couples have an $E_{1/2}$ of ∼−196 mV and ∼−195 mV vs NHE at pH 2, respectively, so reduction under the conditions existing in the protooceans would have been much more favorable. The cyclic voltammetry and EPR spectroscopy of Ti citrate solution with respect to pH suggested the presence of different protonated species existing at the various pH values. The mass spectrometry presented evidence for the coordination of Ti in reduced +3 oxidation state to be different from the one in +4 oxidation state. The evidence suggests that Ti(III) prefers to bind only 2 citrate molecules, where each of them acts as a tridentate ligand. The triplet state EPR spectrum of solid complex **3** presented evidence for the Ti^{III}_2 oxidation state of the complex. The antiferromagnetic coupling between the two metal centers was determined to be -37.2 cm^{-1}.

Acknowledgment. We are grateful to Professor Gary Brudvig for the helpful discussions regarding the EPR spectra. We also thank Dr. James McEvoy for his help with cyclic voltammetry. Acknowledgment is also made to the donors of the Petroleum Research Fund, administered by the American Chemical Society, and the Research Corp.'s Research Innovation Award RI0961, for partial support of this research. This research was also supported by funds from Yale University, Department of Chemistry, and through a DuPont Corp. Aid to Education grant.

Supporting Information Available: Cyclic voltammograms for complex **2** at pH 7 and 8, for complex **1** at pH 6.67, and for Ti(III) citrate at pH 5.3 and 7, a plot of redox potential of Ti(IV) citrate vs pH, a speciation diagram for Ti(IV) citrate solution, ESI-MS of the Ti(III) citrate solution showing the 1:3 Ti/cit species, IR spectra for complex **3** and EPR spectra for the frozen solution of complex **3** at different temperatures, a Curie plot for the frozen solution, EPR spectra for solid complex **3** at 7 K, and the CIF file for the X-ray crystal structure of complex **3**. This material is available free of charge via the Internet at http://pubs.acs.org.

IC051714J

(65) Jungst, R.; Sekutowski, D.; Davis, J.; Luly, M.; Stucky, G. *Inorg. Chem.* **1977**, *16*, 1645−1655.